RESEARCH ARTICLE



Check for updates

Developmental Dynamics WILEY

Lung injury in axolotl salamanders induces an organ-wide proliferation response

Tyler B Jensen | Peter Giunta | Natalie Grace Schultz | Jackson M Griffiths | Timothy J Duerr | Yaa Kyeremateng | Hilary Wong | Adeleso Adesina | James R Monaghan ⁶

Department of Biology, Northeastern University, Boston, Massachusetts

Correspondence

James R Monaghan, Northeastern University, 360 Huntington Avenue Boston, 134 Mugar Hall, MA 02115, USA. Email: j.monaghan@northeastern.edu

Funding information

Northeastern University

Abstract

Background: *Ambystoma mexicanum*, the axolotl salamander, is a classic model organism used to study vertebrate regeneration. It is assumed that axolotls regenerate most tissues, but the exploration of lung regeneration has not been performed until now.

Results: Unlike the blastema-based response used during appendage regeneration, lung amputation led to organ-wide proliferation. Pneumocytes and mesenchymal cells responded to injury by increased proliferation throughout the injured lung, which led to a recovery in lung mass and morphology by 56 days post-amputation. Receptors associated with the Neuregulin signaling pathway were upregulated at one and 3 weeks post lung amputation. We show expression of the ligand, *neuregulin*, in the I/X cranial nerve that innervates the lung and cells within the lung. Supplemental administration of Neuregulin peptide induced widespread proliferation in the lung similar to an injury response, suggesting that neuregulin signaling may play a significant role during lung regeneration.

Conclusion: Our study characterizes axolotl lung regeneration. We show that the lung responds to injury by an organ-wide proliferative response of multiple cell types, including pneumocytes, to recover lung mass.

KEYWORDS

compensatory, ErbB, Nrg1, pneumocyte, regrowth

1 | INTRODUCTION

Injury to the human lung has few therapeutic interventions. Physicians must rely on mechanical ventilation and assistive oxygen therapy until symptoms diminish and the patient can recover some lung function. While there has been evidence of compensatory growth after injury in murine, canine, and human lungs, restoration of lung surface area, and tissue mass can take over a decade in humans. ²⁻⁴ Studying animals with enhanced

regenerative abilities provides the unique opportunity to identify strategies that facilitate regeneration, with the hope of using this information for therapies. The axolotl salamander, *Ambystoma mexicanum*, and several other urodele species have been a focus of research for centuries because they exhibit enhanced regenerative abilities of organs and body parts.⁵ Extensive research has been conducted on axolotl appendage regeneration (limbs and tails) and a few organs (eye, central nervous system, heart, and reproductive system). Yet, there is no evidence

as far as we know of their abilities to regenerate lung tissue. 6 In this study, we determine whether the axolotl regenerates lung tissue after amputation of the distal portion of one lung.

Although axolotls are paedomorphic with a completely aquatic lifestyle, they retain functional lungs used for oxygen exchange. Studies of a closely related adult paedomorphic salamander species, Ambystoma tigrinum, showed that approximately 45% of oxygen uptake occurs through the lungs, which increases under hypoxic conditions.⁷ Like all amphibians, axolotl lungs are less complex than their mammalian counterparts, consisting of a large lumen lined with an epithelium containing a single type of pneumocyte (in contrast to AT1 and AT2 pneumocytes in mammals), goblet cells, ciliated cells, and neuroepithelial endocrine cells.8-11 Epithelial cells cover septa consisting of a pulmonary vein, capillaries, connective tissue, and smooth muscle cells that together generate considerable surface area for oxygen exchange. Considering axolotls also respire through their gills, skin, and buccalpharyngeal surface, the lungs provide a useful organ to study regeneration without significantly impacting animal health.

Regeneration in vertebrates generally occurs either through the generation of a blastema, proliferation throughout the organ, or a combination of the two. The regenerating salamander limb is an example of blastemabased regeneration, whereby a mass of lineage-restricted proliferating cells is formed at the amputation stump and facilitates restoration of a near-identical limb. 12 A feature of blastema-based regeneration is that the new structure derives mainly from cells located at the amputation stump. In contrast, mammals respond to the removal of one lung through an organ-wide proliferative response of contralateral lung called compensatory regeneration, 13 which also occurs in the mammalian liver. 14 Axolotls utilize a similar organ-wide proliferative response after injury of some internal organs, such as, the liver¹⁵ and ovary. 16 Considering the axolotl displays examples of both epimorphic and compensatory regeneration, it is unclear which strategy it would use after lung amputation.

The mammalian lung is a complex tissue containing over a dozen cell types, so it is unlikely that a single endogenous stem cell population generates all cell types. 17,18 The response to partial pneumonectomy in mice (removal of one lung) is widespread with transcriptional changes and proliferation of endogenous epithelial, connective tissue, endothelial, and blood cell types. 19-23 The molecules that enhance compensatory lung regeneration after pneumonectomy are as numerous as the cell types in the lung, including FGF,²⁰ HB-EGF,²⁴⁻²⁶ VEGF,²⁶ retinoic acid,²⁷ SDF1,²⁸ KGF,²⁹ Yap,³⁰ with other signaling pathways involved in chemically-induced injury models.¹⁸ Signaling through the epidermal growth factor receptor family (ErbB) is associated with proliferation of epithelial cells in development, cancer, and after injury. 24,25,31-34 However, the level to which ErbB signaling exacerbates lung injury or promotes regeneration is still debated (35 for review). There are four known ErbB family members, ErbB1-4, with ErbB1 referred to as EGFR. Each ErbB receptor has distinct ligand-binding regions and intracellular pathways that they can activate.³⁶ Among the family members, ErbB2 does not bind ligands, gaining specificity through its heterodimer ErbB binding partner.³⁷ Once activated by extracellular ligand binding, ErbB receptors homo/heterodimerize to mediate cell proliferation and differentiation.³⁸

The ErbB3 ligand, Neuregulin-1 (Nrg1), has been shown to induce proliferation in human lung epithelial cells in vitro via activation of the JAK-STAT pathway. 33,39 Alternatively, Nrg1 can also bind ErbB4 receptors to activate the Hippo-Yap pathway, which has recently been implicated in promoting and controlling epithelial proliferation in the adult rat lung. 40,41 Notably, interleukin-1β has been shown to induce shedding of Nrg1, potentially providing a mechanism through which Nrg1 may give rise to proliferation after injury.⁴²

In this study, we tested whether axolotls are capable of lung regeneration after amputation. We show that axolotls have an organ-wide proliferative response, including the contralateral lung, rather than generate a blastema on the end of the amputated lung. Based upon our recent observation that Nrg1 signaling through ErbB2 receptors was important for axolotl limb regeneration⁴³ as well as the significance of ErbB signaling in mammalian lung regeneration, we set out to determine if Nrg1 and ErbB signaling are involved in axolotl lung regeneration. We observed that ErbB receptors are upregulated after lung amputation, Nrg1 is expressed in the lung and nerves innervating the lung, and show that supplemental Nrg1 induces cell proliferation throughout the lung.

2 RESULTS

2.1 | Characterization of the adult axolotl lung

The axolotl lung is a sac-like structure with a central lumen lined with alveolar septa, similar in structure to other amphibians 11,44 (Figure 1(A)-(C')). The amount of connective tissue varies widely across animals, but the underlying structure and cell composition are typical (Figure 1(A)-(B')). Alveolar septa are covered with ciliary cells on the region nearest the lumen (Figure 1(B')) with

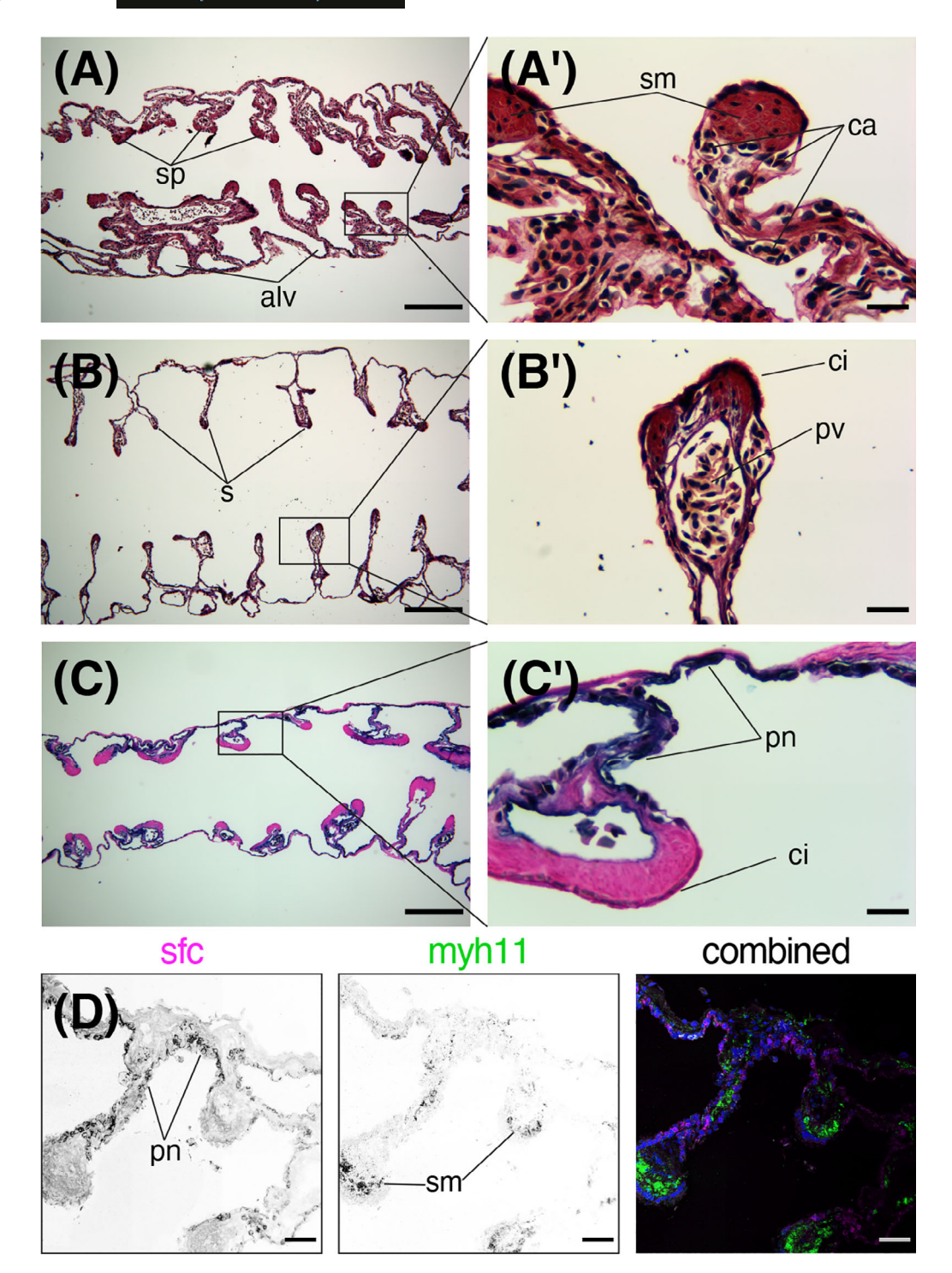


FIGURE 1 Histology of uninjured axolotl lung. (A-B') Masson's Trichrome stained sections of uninjured lungs. Lungs in A and B are from different animals to show variation in levels of connective tissue between lungs. (C-C') Alkaline phosphatase/Eosin stain of axolotl lung showing staining of blood cells and pneumocytes. (D) HCR FISH of uninjured lung showing pneumocytes and smooth muscle. Scale bar in zoomed out images A-C = 500 um. Scale bar in zoomed in images A'-C' = 50 um. sp, septa; alv, alveoli; sm, smooth muscle; ca, capillaries; ci, ciliary cell; pv, pulmonary vein; pn, pneumocyte

goblet cells sparsely dispersed, although these were not stained for in this study.^{8-11,44} No cartilaginous nodules are observed as in other amphibians⁴⁵ (Figure 1(A)-(C'), (D)). Histology shows connective tissue surrounding a

pulmonary vein and capillaries in each septa (Figure 1 (B')). Hybridization chain reaction mRNA FISH (HCR) shows that alveolar septa contain smooth muscle cells expressing myosin heavy chain 11 (Figure 1(D)).

Pneumocytes line the sides and base of the alveolar septa based upon alkaline phosphatase activity (Figure 1(C), (C')) and expression of *surfactant c* (*sfc*; Figure 1(D)).

2.2 Response to lung amputation

We amputated the distal tip of the left lung to characterize the injury response and determine whether regeneration occurs through the generation of a blastema or organ-wide proliferation (Figure 2(A)). All animals survived the surgery, although 20% of animals showed signs of a pneumothorax-type response with air present in the peritoneal cavity over the first 3 days post amputation (dpa). By 3dpa, a clot formed and closed off the wound, which continued to decrease in size over the first 7 dpa (Figure 2(B)-(D')). The wound was covered with an epithelial layer by 7 dpa (Figure 1(D), (D')), which coincided with increased extracellular matrix deposition near the wound site (Figure 1(C)-(E')). An example of likely alveolar neogenesis is shown in Figure 1(E) and (E'). No blastema-like structure was observed in the tissue, and lungs recovered to near-normal morphology by 42 dpa (Figure 1(F), (F')).

Gross lung morphology and size was recovered by 56 dpa (n = 8; Figure 1G). The amount of tissue that regenerated was estimated by measuring the mass of tissue removed during surgery and normalized to body weight (0 dpa), which was used to predict the size of the lung if no regeneration occurred. This estimate was compared to actual total lung mass and the contralateral uninjured lung mass at 56 dpa (Figure 1(H); [P = 0.02]). No statistical difference in mass was observed between the injured left and contralateral right lung at 56 dpa. Together, this suggests that pulmonary tissue was able to recover significant mass in response to amputation through increased growth rates in the injured lung.

Cell proliferation during lung regeneration

To determine if regeneration is associated with cell proliferation near the amputation or throughout the lung, DNA synthesis was measured using 5-ethynyl-2'deoxyuridine (EdU) incorporation (Figure 3(A), (B)). At 21 dpa, cell proliferation increased from baseline throughout the lung up to at least 8 mm away from the injury (Figure 3(B)-(C); EdU). This shows that amputation induces a widespread response throughout the organ rather than localized to the amputation plane or a blastema. HCR FISH along with EdU incorporation analysis showed proliferating sfc⁺ pneumocytes in injured and

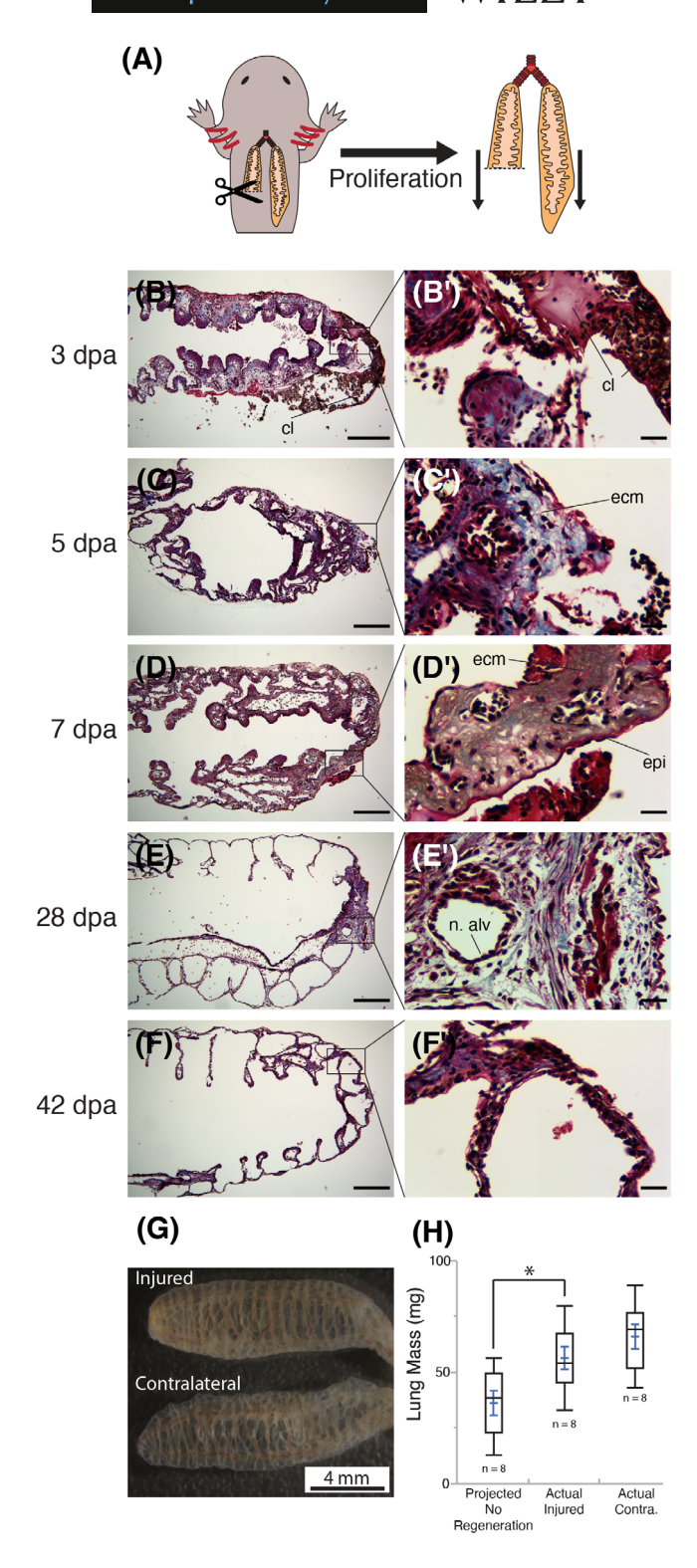


FIGURE 2 Histology of regenerating axolotl lung. (A) Experimental diagram of surgeries. Left lung was surgically injured while right lung was left intact. (B-F") Masson's Trichrome stains of the lung at 3, 5, 7, 28, and 42 dpa. (G) Representative image of injured (top) and contralateral (bottom) lungs at 56 dpa. (H) Lung mass after regeneration of the amputate lung (middle) relative to the contralateral lung (right). Scale bar in zoomed out images B-F = 500 um. Scale bar in zoomed in images B'-F' = 50 um. epi, epithelial cell; cl, clot; ecm, extracellular matrix; n. alv, new alveoli

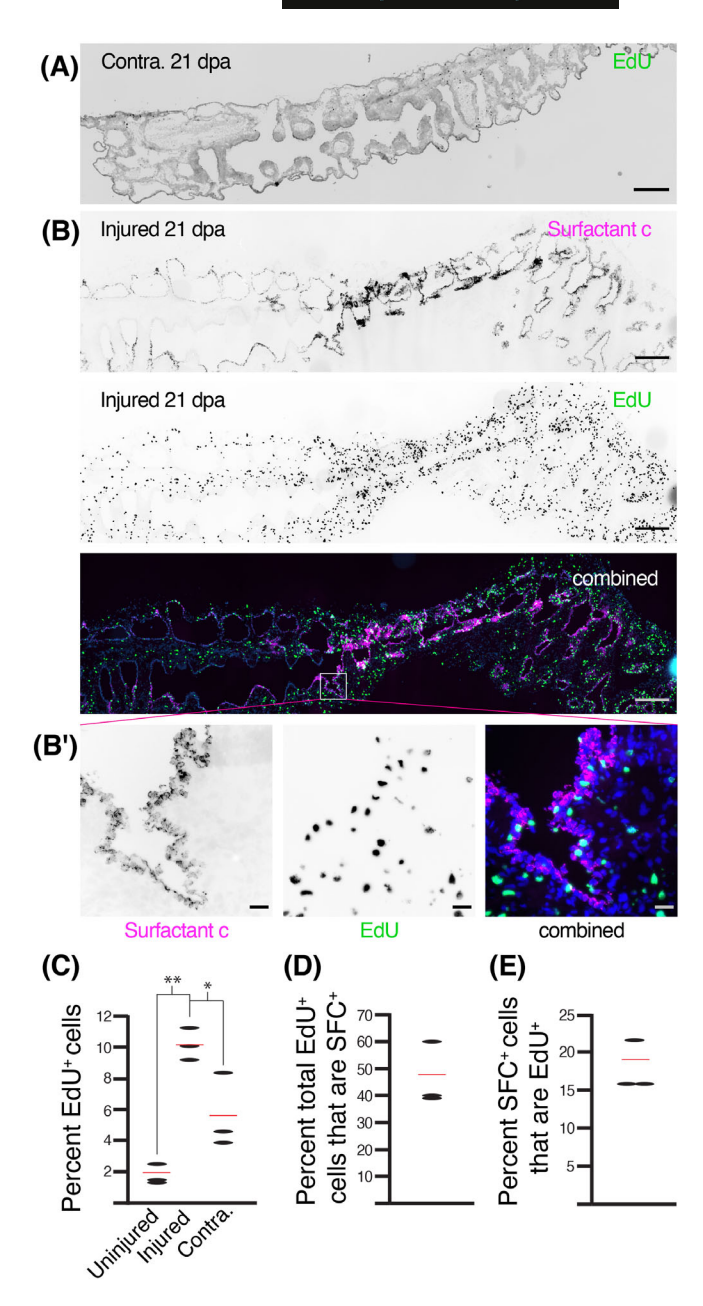


FIGURE 3 Cell proliferataion during regeneration. (A) EdU staining of a contralateral, right lung 21 dpa of the left lung. (B) HCR FISH for *sfc* and EdU staining of an injured left lung 21 dpa. (B') Close-up image of a region in B. (C-E) Graphs showing cell counts in injured vs uninjured lungs. Scale bar in zoomed out images A-B = 500 um. Scale bar in zoomed in images B' = 25 um

contralateral lungs (n = 3; Figure 3(A)-(B')) although both sfc^- epithelial cells and mesenchymal cell types proliferated during regeneration.

The average number of EdU⁺ cells was 5.25-fold higher in injured lungs (10.1%; n = 3) vs lungs from uninjured animals (1.9%; n = 3; P = 0.002) and 1.83-fold higher compared with contralateral lungs in injured animals (5.5%; Figure 2(C); P = 0.032). At 21 dpa, 46.8% of EdU⁺ cells were sfc^+ expressing pneumocytes (Figure 3

(D)), while 18.0% of pneumocytes were EdU⁺ (Figure 3 (E)). These result show that approximately half of dividing cells are the gas-exchanging pneumocytes while the rest are either other epithelial cell types, smooth muscle, connective tissue, or endothelial cells (For example see Figure 3(B')). Together, this shows that regeneration is an organ-wide response that utilizes proliferation of multiple cell types in order to regain mass lost from amputation. Although proliferation was observed in the uninjured contralateral lung, it was not significantly higher than uninjured lungs suggesting that the injured lung is growing faster than the contralateral lung.

2.4 | Nrg1/ErbB signaling during regeneration

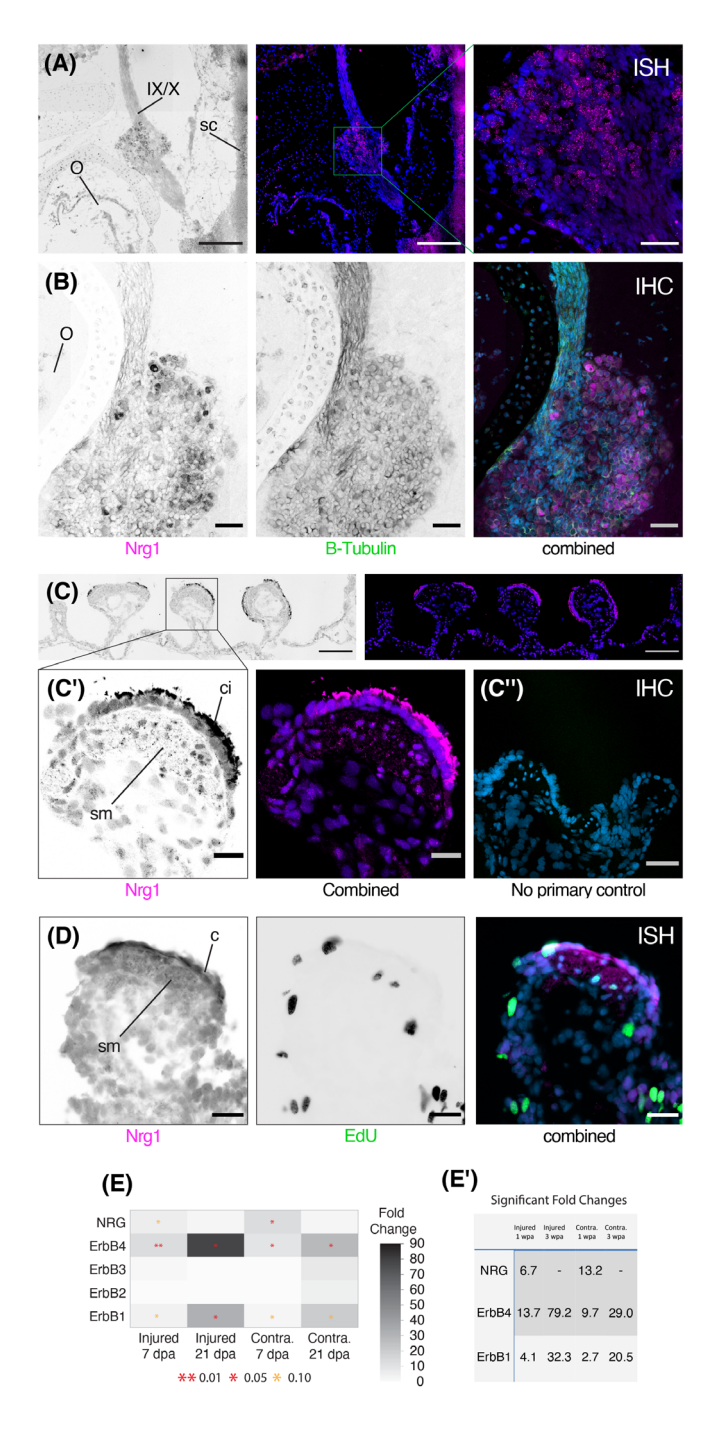
We reasoned that pathways involved in mammalian lung development and repair including Nrg1/ErbB signaling might also be utilized in axolotl lung regeneration. We first used HCR and immunohistochemistry to localize *nrg1* mRNA and Nrg1 protein in cranial nerve IX/X ganglion, which innervates the lungs among other organs (Figure 4(A) and (B)). Nrg1 mRNA and protein was also observed in the lung septa at 21 dpa in regions enriched with ciliated cells as well as smooth muscle cells (Figure 4(C) and (D)). Together, these observations suggest that Nrg1 ligand might be provided by both nerves innervating the lung as well as cells within the lung.

We next determined if members of the Nrg1/ErbB signaling pathway were upregulated during regeneration. We examined *nrg* and *erbb1/2/3/4* mRNA expression at 7 (n = 3) and 21 (n = 4) dpa and found that *erbb1* and *erbb4* expression were increased at all time points, while the ErbB ligand, *nrg1*, was upregulated at 7 dpa (Figure 4 (E), (E')). In mammals, ErbB2/ErbB4/Nrg signaling is implicated in activation of proliferative genes, and can serve multiple roles in lung tissue, ⁴⁶ while ErbB1 activation is implicated in promoting differentiation and enhancing pneumocyte maturation. ⁴⁷ This observation suggests that signaling through ErbB receptors might be involved in the proliferative response associated with lung regeneration.

2.5 | Supplemental administration of Nrg1

Considering Nrg1's ability to activate ErbB2, ErbB3, and ErbB4, we set out to determine if systemic administration of Nrg1 peptide could induce cell cycle re-entry in uninured lungs. Uninjured animals were injected intraperitoneally with recombinant Nrg1 peptide (n = 7;

100 ng/g body weight) (Figure 5(A)). Nrg1 administration caused a 3.9-fold increase in total EdU+ cells compared to sham-injected controls (P = 0.003; Figure 5(B)-(C)). The epithelial layer (Figure 5(D)) had a 4.18-fold increase (P = 0.006), while the mesenchyme showed a 3.74-fold increase, but was not to statistically significant levels (P = 0.056). Transcript levels for *erbb4*, *erbb3*, and *erbb1* were significantly increased after Nrg1 administration similar to those observed in amputated lungs suggesting that a similar regenerative response may be occurring (Figure 5(E)). These observations suggest that Nrg1



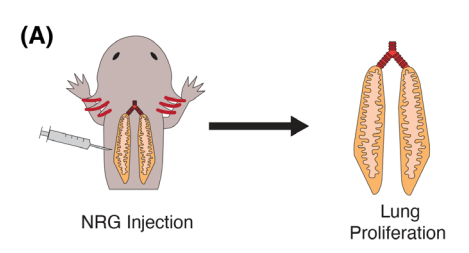
ligand induces a proliferative response in the uninjured axolotl lung and activates Nrg1/ErbB signaling genes in a similar manner to lung amputation.

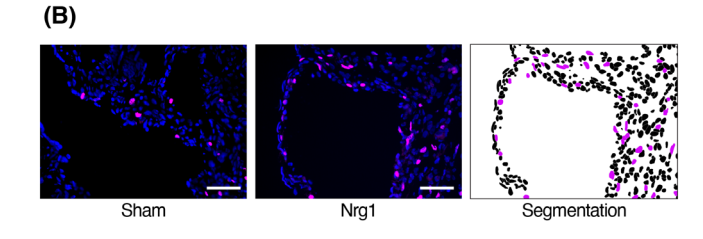
3 DISCUSSION

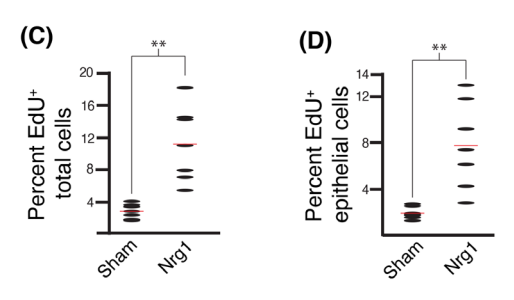
This study provides evidence that the axolotl salamander is capable of significant lung regeneration after amputation. Rapid wound closure occurred after amputation, which led to induction of DNA synthesis and recovery from injury by 56 days post amputation. During salamander limb regeneration, proliferation occurs within the proximity of the injury site and contributes to the formation of a blastema. It appears that lung regeneration is mechanistically distinct from the regenerative response that occurs in the limb by inducing growth throughout the injured organ. We also found that proliferation was higher in the injured lung compared with uninjured contralateral lungs suggesting that growth of the injured lung is higher than the uninjured lung to compensate for the missing tissue.

Cell proliferation was observed in a number of cell types including cells resembling pneumocytes, ciliated cells, smooth muscle cells, and connective tissue/fibroblast cells. Our current understanding of the mammalian lung is that lungs contain a number of facultative progenitor cells that are quiescent, which become proliferative after injury. 17 Our study shows a similar response in axolotls suggesting that regeneration after injury occurs by proliferation of multiple cell types to coordinate a regeneration response, similar to what occurs in damaged mammalian lungs.

FIGURE 4 Expression of genes associated with Nrg1/ErbB signaling. (A) HCR FISH for nrg1 in the IX/X cranial nerve and in the spinal cord. Scale bar = 500 um. Inset = 100 um. (B) Immunohistochemistry of Nrg1 and acetylated beta-Tubulin staining cell bodies and axons of peripheral nerves. Scale bar = 100um. (C-C') Immunohistochemistry of Nrg1 in the injured lung 21 dpa. Notice expression in ciliated cells and smooth muscle cells. (C") No primary control immunohistochemical stain. Scale bar in C = 250 um. Scale bar in C' = 50 um. Scale bar in C'' = 100um. (D) HCR FISH of nrg1 and EdU staining in the injured lung 21 dpa. Notice proliferation in both epithelial and mesenchymal cell types. (E) Heat map of qPCR fold increases at both 7 dpa (n = 3) and 21 dpa (n = 4) for the left (injured) and right (contralateral) lungs. Red asterisks denote significant upregulation of mRNA products (P < 0.05), while orange asterisks denote trending toward significance (P < 0.10). (E') Table of significant fold changes (P < 0.05) for the qPCR results with fold changes indicated. IX/X, IX/X cranial nerve ganglion; o, optic cup; sc, spinal cord







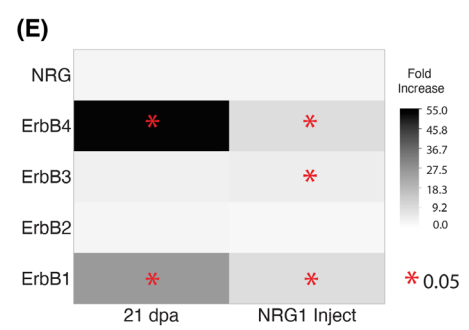


FIGURE 5 Cell proliferation in the lung after Nrg1 administration. (A) Representative experimental outline. Lungs were left intact and Nrg1 peptide was injected I.P. into animals (n = 7). (B) Representative images of sham (PBS-injected) and Nrg1 injected animals (middle) used for cell segmentation (right) and cell counts in (C) and (D). (E) Heat map of qPCR fold increases after injection of NRG (n = 4) as compared with control (n = 4). Red asterisks denote significant upregulation of mRNA products (P < 0.05)

We observed upregulation of receptors *erbb1* and *erbb4* at both 1 week and 3 weeks after distal amputation in the lung, as well as an upregulation of the signaling ligand *nrg1* at 7 dpa. ErbB1 has been implicated in promoting lung cell maturation and differentiation, ⁴⁷ and a ligand of ErbB4, Nrg1, has been shown to play an important role in lung development. ^{48,49} When used to activate ErbB4, Nrg1 can control both lung epithelial cell proliferation and surfactant synthesis in vitro in mammalian

pulmonary cells. 46 ErbB2 plays an important role in Nrg1 signaling, and its loss halts proliferation and regeneration in many tissue types. 50-52 It is also known that once ErbB4 is activated, it can undergo proteolytic cleavage and release its intracellular domain to regulate cell signaling.53 This would indicate that Nrg1 signaling to ErbB4/ErbB2 heterodimers could be controlling pulmonary cell proliferation during regeneration, although we did not rule out that Nrg1 could signal through ErbB3/ ErbB2 heterodimers. We also did not rule out that Nrg1/ ErbB signaling is downstream of other signaling pathways that are inducers of lung regeneration. In human patients after acute lung injury, physicians have noted elevated Nrg1 levels in bronchoalveolar lavage. 42 This would lead to the conclusion that this pathway is present in human lung tissue and warrants further study.

We have demonstrated that IP injection of exogenous Nrg1 peptide is sufficient to induce a proliferative response, partially mimicking the response seen after injury. We show that at least two possible sources for Nrg1 exist including the IX/X cranial nerve that innervates the lung and cells within the lung including ciliated cells and smooth muscle. Further study is required to show that nerve-derived Nrg1 ligand is required for lung regeneration. It is also unclear whether Nrg1 signaling is directly acting on all proliferating cells in the lung. It is highly likely that Nrg1 is activating a subset of cells that then undergo paracrine signaling with surrounding cells to promote cell proliferation. It is also likely that these secondary signaling events utilize other signaling pathways. Furthers studies are needed to understand the dynamics of cell-cell communication during the lung regeneration response.

In conclusion, we have provided the first glimpse at how this model organism regenerates its lung tissue and provide a basis for further research into the molecular mechanisms driving lung regeneration.

4 | EXPERIMENTAL PROCEDURES

4.1 | Model and subject details

Axolotl procedures were approved by the Northeastern University IACUC. All experimental procedures and animal care were conducted in accordance to vertebrate care guidelines. Animals were on average 13 cm in total length and 7 cm in snout to vent length, 6 months old, and were raised in Northeastern University lab facilities according to.⁵⁴ Animals were kept in individual tanks with regular water changes and fed soft salmon pellets 3 times a week. Sample size was selected after seeing a large effect size in preliminary data. No exclusion criteria

were determined: all animals were included. Animals were non-randomly assigned to groups to ensure all animals were at the same stage of development.

4.2 Surgical procedures

Axolotls were sedated by immersion in 0.01% benzocaine solution. An incision was made above the spleen on the left flank. Forceps were then inserted into the abdominal cavity through the small hole, passing beneath dorsal muscles running parallel to the spine. The distal lung tip was pulled through the incision, and approximately the distal third of the lung was amputated using dissecting scissors. Forceps were then used to push the remaining lung tissue away from the incision to prevent tissue adhesion at the wound site. The wound was then closed with 3 M Vet Bond tissue adhesive. The axolotl was placed back into animal housing with daily observation to check recovery progress.

4.3 Tissue processing and histology

The flank of euthanized animals was opened using dissecting scissors and right and left lungs removed. An insulin syringe was used to inflate lungs with 10% neutral buffered formalin while forceps were used to seal the bronchial openings. Lungs were then submerged in 10% neutral buffered formalin and fixed overnight at 4°C. After fixative treatment, lungs were washed in phosphate buffered saline (PBS) 3 times and immersed in 70% ethanol. Tissues were processed for paraffin embedding and sectioned at 8 um. Slides were heated at 55°C for 1 hour to adhere wax sections to the slides prior to deparaffinization and staining. Tissues underwent either Masson's Trichrome Straining (Thermo Scientific Chromaview) or incubated in BM Purple (Roche) overnight at 4°C followed by eosin stain to detect alkaline phosphatase activity. Imaging was performed on a Zeiss Axiozoom V16.

4.4 | Hybridization chain reaction in situ hybridization

Probes were designed using Oligominer⁵⁵ and filtered to ensure specificity to the target gene using Bowtie 2⁵⁶ genome^{57,58} axolotl (https://github.com/ davidfstein/probegenerator). Split initiator sequences were appended to the probes according to version 3 HCR.⁵⁹ Probes were designed for sfc (25 probe pairs), myh11 (36 probe pairs), and nrg1 (31 probe pairs), and ordered as 50 pmol/oligo pools (Table 1; oPools; Integrated DNA Technologies). Probes were resuspended at 1 uM concentration in 1× TE solution (IDTE; Integrated DNA Technologies).

Extracted lungs were inflated with a 1:1 mixture of optimal cutting temperature medium and PBS, immediately snap frozen, and stored at -80°C. Tissues were cryosectioned at 10 um, immediately frozen at -20°C for 30 minutes in the cryostat and then fixed in 4% paraformaldehyde at room temperature for 10 minutes. Sections were washed 3 times for 5 minutes each in 2x salinesodium citrate buffer (SSC) followed by 2, 5 minute incubations in 4% SDS, 200 mM boric acid, pH 8.5. Sections were then washed 3 times in 2xSSC for 5 minutes each followed by 10 minutes in 100% ethanol. Sections were washed 2 times for 5 minutes each in 2xSSC and prehybridized with hybridization buffer (Molecular Instruments) for 15 minutes at 37°C. Probe pools at 5 nM final concentration in hybridization solution were added to each slide and hybridized overnight at 37°C. Three probe washes were performed in Molecular Instruments probe wash at 37°C for 15 minutes each, followed by 5xSSC with 0.1%Tween-20 (5xSSCT) for 15 minutes at 37°C, and finally 5 minutes in 5xSSCT at room temperature.

Probe detection was performed by incubation in amplification Instruments 10 minutes. Fluorescently-labeled hairpins (Molecular Instruments) were prepared by heating to 95°C for 90 seconds and left to cool to room temperature for 30 minutes in the dark. Hairpins were diluted 1:50 in amplification buffer, added to sections, and incubated overnight at room temperature in the dark. Sections were then washed twice for 30 minutes each in 5xSSCT. Sections were either immediately stained with DAPI and mounted in Slowfade TM Gold (Thermo Fisher) for imaging or processed for EdU click chemistry. Confocal images were taken using a Zeiss LSM800 laser scanning microscope. Figures 3(A), (B), (C) were taken using a Zeiss Axiozoom V16 microscope.

4.5 | Cell proliferation analysis and **Immunohistochemistry**

Cell proliferation analysis was performed by intraperitoneally injecting EdU (100 ng/g of animal weight, Click Chemistry Tools) 3 hours prior to tissue collection. After HCR, sections were incubated for 30 minutes at room temperature in Click-chemistry mix consisting of final concentrations of 1x TRIS buffered saline, 4 mM CuSO4, 2uM AFDye 594 Azide (Click Chemistry Tools), and 100 mM Sodium Ascorbate. Slides were then washed in

HCR FISH probes
王
and nrg1
Ļ,
\overline{z}
, myh1
sfc,
for
ligos
0
_
H
Ä
TABI
⋖
Ε

sf cB3 initiator	myh11 B1 initiator	nrg1 B3 initiator
gTCCCTgCCTCTATATCTTTTCAGGGCGCATGGAGCTGGTCAGGT	gAggAgggCAgCAAACggAAGCCACTGGGGCTGTTAATAAAGTTTT	gTCCCTgCCTCTATATCTTTGCTGACTAGGCAAGCGACGATGGGC
CAGAGCGTGCCTTTTATAGCGCAGGTTCCACTCAACTTTAACCCg	AGTTTCTTAGCTGACCAGTCAGCCTTAgAAgAGTCTTTCCTTTACg	CTTGAGGCCAGCAATGCAGAGGCAATTCCACTCAACTTTAACCCg
grccctgcctctatatctttgtgcccgggctctgtgccactcctc	gAggAgggCAgCAAACggAACTCCCTTAGATTGTGCAGCACTGAC	gTCCCTgCCTCTATATCTTTGTGGGTAGGGGAATCGTATTCAAAA
GCGTCCAACGTTCTTTCGATCCTGTTTCCACTCAACTTTAACCCg	CGTATAAATGAGCCCGGAGAAGTATTAgAAgAgTCTTCCTTTACg	ATCTTGGCCTATCCTGCCTGGGTCATTCCACTCAACTTTAACCCg
gTCCCTgCCTCTATATCTTTGGCTTCTTTGCCGCCGTTCCCCATC	gAggAgggCAgCAAACggAATTCACCCGTGCACAGAATGGACTGG	gTCCCTgCCTCTATATCTTTCGAAGCAGAGTCGACATAAATAATC
TGCGTAGAGCGGAGGACTGTCCATTTCCACTCAACTTTAACCCg	CGTGTTCTCAGTTTTGCCGGCACCATAgAAgAgTCTTCCTTTACg	AGTGGAGCTTGGGACCAAGGGAGGATTCCACTCAACTTTAACCCg
gTCCCTgCCTCTATATCTTTGCAGGGGATCTTGGGCACTGGGAAA	gAggAgggCAgCAAACggAAGTCAAAGTTGATCCGGATGAATTTA	gTCCCTgCCTCTATATCTTTACTGATGGCAGAGCTGGGCATCGGA
GAGCAGCTTCTTGAAGTGGATGGGGTTCCACTCAACTTTAACCCg	ATTGGCTCCAACAATGTAGCCAGTCTAgAAgAgTCTTCCTTTACg	CGGCTCTGCTTGCACGGCCCCTTGATTCCACTCAACTTTAACCCg
gTCCCTgCCTCTATATCTTTGATGAACACGACGACCAGGACGATG	gAggAgggCAgCAAAACggAAACGGACGACACAACCTTCATCATGG	gTCCCTgCCTCTATATCTTTAGAGGCACCGAGGGCTCAGATGGGG
CAGGATGGCCACCACGATGACGATCTTCCACTCAACTTTAACCCg	TTGAAGACGATGTTGCCCAGCTGCATAgAAgAgTCTTCCTTTACg	TCGGGAACCATGCCCTCTGGAGTGGTTCCACTCAACTTTAACCCg
gTCCCTgCCTCTATATCTTTGTGCTTCTGGGTCATGAAGAGCCCC	gAggAgggCAgCAAACggAAGCCAGAGCTTCTATAGCAAAGTCCG	gTCCCTgCCTCTATATCTTTGTTTGCACAGGAATGGCCGTCGTGG
GAGGGACATCTGGAAAATGCTCTCGTTCCACTCAACTTTAACCCg	AGGAAGAGGCGCTCGTATGTTGCCTTAgAAgAgTCTTCCTTTACg	CTGGCAGTTTGCAGATTGGTTTCTGTTCCACTCAACTTTAACCCg
gTCCCTgCCTCTATATCTTTCTGCGAGTCCTTCCCATCCGGGCCA	gAggAgggCAgCAAAACggAAGGCCGAAGTCGATGAAGCTCCACTC	gTCCCTgCCTCTATATCTTTATGGTCGGTGTAGTTGTCAGGTGTT
TTCCTTCCGGTCTGTGGGCAGCCTCTTCCACTTTAACCCg	TCAGCTCGATGCAAGGCTGCAGATCTAgAAgAgTCTTCCTTTTACg	TTGCATTTTATAAGATGCCCTGTTCTTCCACTCAACTTTAACCCg
gTCCCTgCCTCTATATCTTTACTGCGGATGTAGAACGTGGCGACG	gAggAgggCAgCAAAACggAAGCACTAGCGTTGTAGTCCACCTTTC	gTCCCTgCCTCTATATCTTTTCACGCAGTAACTCCTCTGATTTT
CACCACCGTGGCCGAGCTGTTGACTTTTCCACTCAACTTTAACCCg	AGCGGGTCCATGTTCGTCAGCCTAgAAgAGTCTTCCTTTACg	TCCTTGAGGACAAAGCACTCGCCACTTCCACTTTAACCCg
gTCCCTgCCTCTATATCTTTAGCACGCCCGTCCAGGCCAGG	gAggAgggCAgCAAAACggAAGTCAGCTGCTCCTTGTACAGCTGCC	gTCCCTgCCTCTATATCTTTCACACATATTTTGTACTGCTCGTAA
TGTCGTCCTCGTCCATTTTGCTGATTTCCACTCAACTTTAACCCg	GTGTTCCTGAGGGTGGTCATGAGCTTAgAAgAgTCTTCCTTTACg	TCACCAGTAAACTCATTTGGGCACTTTCCACTCAACTTTAACCCg
gTCCCTgCCTCTATATCTTTCCTTGGTGATGGCCTCCAGGCTGGG	gAggAgggCAgCAAAACggAACCGGCAGCAAGGATCTCGTACCGCT	gTCCCTgCCTCTATATCTTTCTGGCCATTACGTAGTTTTGGCAGC
GGGGCTTACTCTCCATGTTCTGAAATTCCACTCAACTTTAACCCg	CCGTCCATGAATCCTTTGGGAATATTAgAAgAgTCTTCCTTTACg	AATTCAATCCCAAGATGCTTGTAGATTCCACTCAACTTTAACCCg
gTCCCTgCCTCTATATCTTTGGTGACCGGGGTGGCCTCGCTCTCT	gAggAgggCAgCAAACggAAAACGCCTTTCTGGCGAGGTAGCCCC	gTCCCTgCCTCTATATCTTTTTCTGATAGAGTTCCTCAGCTTCCA
CGGTATTCTCTTGGTCTGGCAAGGCTTCCACTCAACTTTAACCCg	GCCGTCAGCTGCTGTTGCCGCTTTGTAgAAgAgTCTTCCTTTACg	CAGATGCCAGTTATGGTCAACACTCTTCCACTCAACTTTAACCCg
gTCCCTgCCTCTATATCTTTTGCCCAAGAGTGAGTCTCCCATCCT	gAggAgggCAgCAAACggAAAGTTCCTTCAATTCGCTGTCTGCTT	gTCCCTgCCTCTATATCTTTATGATGCCAACTACAAGGAGGGCAA
GGCCACTGCAAAGGACGCGGACTGTTTCCACTCAACTTTAAACCCg	TCGGAGAGCTGTGTGCTTCTGCTTAgAAgAgTCTTCCTTTACg	TTGGTTTTGCAGTAGGCCACACACTTCCACTTTAACCCg
gTCCCTgCCTCTATATCTTTCTGCTCACTAGGCCCAGATGAGGGG	gAggAgggCAgCAAACggAATGCAGCATCTTCTTCTTCTTCTT	gTCCCTgCCTCTATATCTTTTGCCGAAAACGATCATGCAACTTTT
CCCTCTACAATGTACCACAACATGTTTCCACTCAACTTTAACCCg	AGCTGCTCCTCGAGATCCTGCATTTTAgAAgAGTCTTCCTTTACg	ATGTTGTTCCTTTCAGAGCGTAGGCTTCCACTCAACTTTAACCCg
gTCCCTgCCTCTATATCTTTAGCAGGCAGAGTGTGATGGACACGA	gAggAgggCAgCAAACggAAGAAATCATGGATTCATGCTTGTTTT	gTCCCTgCCTCTATATCTTTTGGTGAGGCCCATTAGCCATGTTTA
GTAAGTAGCGGACACTTCATGGGCATTCCACTCAACTTTAACCCg	TCTTTCTTCAGCCGCACTTCCAGTTTAgAAgAgTCTTCCTTTACg	TGGACGTTTTCTTGGGGTGGATTTGTTCCACTCAACTTTAACCCg
gTCCCTgCCTCTATATCTTTCCGTAAGGCAGAAGGCACCCGCCCC	gAggAgggCAgCAAACggAACGGATTTTCTTGAGGGCGTTGTTTT	gTCCCTgCCTCTATATCTTTTGACACATACTGATTTACCA
TGCATATACAGGACCCCAGTGTAAATTCCACTCAACTTTAACCCg	AGATCAGAGATATGGCCTTCCAATTTAgAAgAgTCTTCCTTTTACg	TCAATGACGTGTTCACTGGATATCATTCCACTCAACTTTAACCCg
gTCCCTgCCTCTATATCTTTAATAAGCCACATTGCAATTACAGTT	gAggAgggCAgCAAACggAATCATCATCTAGCGCCCTCTTCAGCA	gTCCCTgCCTCTATATCTTTGTAGAGAATGATGTTTCGGTTTCTC

TABLE 1 (Continued)

sf cB3 initiator	myh11 B1 initiator	nrg1 B3 initiator
AGTGAATGTGAAGAGGAGCCGTGTTCCACTCAACTTTAACCC	TGGACCTGAGCCTCATGGGCCCGGGTAgAAgAgTCTTCCTTTACg	$\tt TGATGCGTTGTTGAAGTATAGTGACTTCCACTCAACTTTAACCCg$
gTCCCTgCCTCTATATCTTTGATTATTTTATCAACAACCCCTCC	gAggAgggCAgCAAACggAAGTCAGTTGGTTGCGGACACGCTCGC	gTCCCTgCCTCTATATCTTTCTTGGAGTCTGCGTGACTGTTGTAG
GACCAGACAGACAGACAGCTCCTCGTTCCACTTTAACCCg TCCACCTGTAGCTTGTGCGTCTTCTTAgAAgAGTCTTCCTTTAC	TCCACCTGTAGCTTGTGCGTCTTCTTAgAAgAgTCTTCCTTTACg	TCAGACTGGCCGTTGCTCCAGCTGTTTCCACTTTAACCCg
gTCCCTgCCTCTATATCTTTGAGGTACTGCAGAGACACAGAAGCA	gAggAgggCAgCAAACggAATCAAGCTGGTCTTGTAGGCTGTTTT	gTCCCTgCCTCTATATCTTTACGGAGTGACTTTCTGAGATAATGC
TAGCAATCACTTGTGATCTTTAATGTTCCACTCAACTTTAACCCg	AGGTTCTGCTTCCGCTTCCTTAgAAgAgTCTTCCTTTACg	CTGTTTTCCACAGACGATGTCATAATTCCACTCAACTTTAACCCg
gTCCCTgCCTCTATATCTTTAATATGTTTGTAAACTGCTCAATTC	gAggAgggCAgCAAACggAAATCTGATCAAATTTCTTCTGCTTTT	grcctgccrctatatcttrctaggrccggctgggcttgtatgcc
GCAAAATGATTACTTTATTCAAACATTCCACTCAACTTTAACCCg	GAAGAGATGGTTTTCTCCTCGGCAATAgAAgAGTCTTCCTTTACg	GGACCACCAATTCCATTAAGACGTCTTCCACTCAACTTTAACCCg
gTCCCTgCCTCTATATCTTTGGCAGGGAAATGGCACTCTTAGTCA	gAggAggCAgCAAACggAATGAACGTTCTTGCCGACGTCATCTT	gTCCCTgCCTCTATATCTTTTGCCGGAGGAAACTGTTGCAATCAC
GATCGCAGCCTCTCTGGCACCCAATTCCACTCAACTTTAACCCg	AGGCCGCGCTTGGACTTCTCCAGATTAgAAgAgTCTTCCTTTACg	CTGTAGGAGTCTGTCTTTGTTCCACTCAACTTTAACCCg
gTCCCTgCCTCTATATCTTTCACCATGCACACTTTCCAGGAGGT	gAggAggCAgCAAACggAATCATGAACCTGTTTCACCAGCTGCC	gTCCCTgCCTCTATATCTTTACATACCTTTCACTGTGAGGAGAAT
TGGGTACTCACTCGGCACTCATTTTCCACTCAACTTTAACCCg	CGCTCATCTTCCAGTTCTGTTTCGTTAgAAgAgTCTTCCTTTACg	ATTCGAGCTGGTGTCATGGCTGTTCCACTCAACTTTAACCCg
gTCCCTgCCTCTATATCTTTGTTATGCCTTATAGCATTGATCTGT	gAggAggCAgCAAACggAAAAGATCTCTTCTTTGCCGCTCGGG	gTCCCTgCCTCTATATCTTTCAAGGAGTTTGGAAATCCACTGGCG
TCTATCTGAACCACCAATTGAGATCTTCCACTCAACTTTAACCCg	TTCTTTTCATTTTCTCTTGCTGTAgAAAgAgTCTTCCTTTACg	ACCTCTGAAATAGGGGACCTTGGAGTTCCACTCAACTTTAACCCg
gTCCCTgCCTCTATATCTTTCATCTTGCCACTTCCACTACTCG	gAggAgggCAgCAAACggAATCTTCCTCCAGTTGGGAAATTCTGG	gTCCCTgCCTCTATATCTTTACAGTTAGAATGGATACTGGTGGTG
GTCCTTTAGTTGTTTTCTTCACAAGTTCCACTCAACTTTAACCCg	TCCATGTTGCTCTGTTCCTCGTCAATAgAAgAgTCTTCCTTTACg	GGACTGACAGCCACAGAAGGAACCGTTCCACTCAACTTTAACCCg
gTCCCTgCCTCTATATCTTTGAACATTTCCCTTTGTTGAACAGAA	gAggAggCAgCAAACggAAACGGTGGCCTTAAATTTTGGACTTCA	gTCCCTgCCTCTATATCTTTACCTCTTTTCGCGTAGTCGAGGGG
CTTGGCGGAAGGTGGGAAAAGCTTTTCCACTCAACTTTAACCCg	TGTGCAATCTTGGCTTCCAGGGCACTAgAAgAgTCTTCCTTTACg	TGGAATTGCTGGTTGTAGTAATGGTTTCCACTCAACTTTAACCCg
gTCCCTgCCTCTATATCTTTATCTCGCTTGAGTTCCTCTCGGTCC	gAggAgggCAgCAAACggAATCCTCCAGCTGCCTCTTGAGCTGTT	gTCCCTgCCTCTATATCTTTTCATGGACAGGATTGTGGTGGTATG
GACTGCTTCAGAGAAAGATTCTACTTTCCACTCAACTTTAACCCg	TTGATGCGCTGCGACTCTTCCGTAgAAgAgTCTTCCTTTACg	AAAGGACTGGTGGAAGGCTGCTGCTTCCACTCAACTTTAACCCg
	gAggAgggCAgCAAACggAAAGCTCCACCAGCACCTCGTCTCCCT	grcctgccrctatatcttttcatactcttcatcctccactatcc
	ACGGTGATCTTCCCACTGTCCATAgAAgAgTCTTCCTTTACg	TGTATGGGCTCATATTCCTGTGTGGTTCCACTCAACTTTAACCCg
	gAggAgggCAgCAAACggAACTTGTACATCTCTATGATCTTCTCA	grcctgccrctatatcttttgtgaccattttggttttgttctttt
	GGGCGCCATITICGTGCCTTTTTAgAAgAgTCTTCCTTTACg	CAGAGTTCATTTCTAATCGGTTAGATTCCACTCAACTTTAACCCg
	gAggAgggCAgCAAACggAATTCCAGCTCTCCAGTGATGCTGGTG	grcctgccrctatatctttagaatggcgtatcttcacctatttt
	GATGGGGTTGGCTTGAAGAAGCTGCTAgAAgAgTCTTCCTTTACg	TGGTTGCGAGTGGATTTTGTATGCTTTCCACTCAACTTTAACCCg
	gAggAgggCAgCAAACggAAATGGGCACATTTCCTTGGCATAAAA	grcctgccrctatatctttgtcggtatgcagtggctgaatctag
	AACATTTCGCCGTCATCCTGGCCAGTAgAAgAgTCTTCCTTTACg	${\tt TAGTTGGGTTAGTCCTGCTATCAGTTTCCACTCAACTTTAACCC}_g$
	gAggAgggCAgCAAACggAAACATTGATACCTTAAGATGGCAGA	grccrgccrctatatctttgcaagtcttcctgcgtggagaaccg
	GTCAGGATGCACCTTGTGAAATCCGTAgAAgAgTCTTCCTTTACg	TAGCTATTACACTGGAGAGCCTTGCTTCCACTTTAACCCCg
	gAggAgggCAgCAAACggAATGATGCAGAGCTGCTCGAAGGAGTT	grcctgcctctatatctttatgtttatacagcaacagggtcttg
	GCTGCTGAAGCTTCTCGTTGGTGTATAgAAgAgTCTTCCTTTACg	AAGTTTTACAGGTCACTCTATATGTTTCCACTCAACTTTAACCCg

(Continues)

TCAAGGTGCGCCAGGACGCCCGTCCTAgAAgAgTCTTCCTTTACg

gAggAgggCAgCAAACggAATTCACTTTGGTGAAGAGTCTCCACC

CCCTCCAGTACACCGTTGCACCTCATAgAAgAgTCTTCCTTTACg gAggAgggCAgCAAAACggAAAAGAAGACCTTGCTCTGTCCAACTC **ICTIGGCGGGTGACTIGGAGCAGAGTAgAAgAgTCTTCCTTTACg**

1xPBS, 3 times for 5 minutes each. Nuclei were stained with DAPI (Invitrogen) before mounting and imaging.

For immunohistochemistry, cryosections were processed the same as when performing HCR. After fixation, sections were washed in 1xPBS and then serum blocked in 1.5% goat serum for 30 minutes at room temperature. Anti-Nrg1 primary antibodies (ThermoFisher, PA5-13204; 1:1000) were diluted in 1.5% goat serum in 1xPBS and placed on sections overnight at 4°C. Secondary antibodies were diluted in PBS and incubated on sections for 30 minutes (1:500 Life Technologies). Sections were stained with DAPI before imaging.

4.6 | Image quantification

Images were all obtained as single optical slices from confocal imaging and stitched using the Zen Blue 2.6 software. Cell segmentation was performed by extracting the DAPI channel in the FIJI Imaging Package^{60,61} and cell segmentation performed using the deep learning-based Cellpose package.⁶² Masks were imported back into Fiji as regions of interest and manually counted using the cell counter plugin. For presentation purposes, greyscale images were processed by adjusting for brightness and contrast and a Gaussian blur performed with a radius of 2.0.

4.7 | Nrg1 injection

Animals were anesthetized in 0.01% benzocaine and 100 ng of recombinant human Nrg1 β -1 peptide per gram of animal weight per day was injected I.P. for 3 days (Peprotech, 100-03). At 3 days post-treatment animals were injected I.P. with EdU, euthanized 3 hours later, and lungs collected for sectioning and mounting.

4.8 | qPCR analysis

Lungs were collected from animals at one and three wpa, and lungs were flash frozen using liquid nitrogen and stored at -80° C. Total RNA was extracted using TRIzol Reagent (Life Technologies) followed by Qiagen RNeasy kits according to manufacturer's protocol. Samples were transcribed to cDNA using a Verso cDNA Synthesis Kit (Thermo Scientific). qPCR was performed using SYBR Green Supermix (Applied Biosystems) with cDNA generated from 25 ng total RNA and 0.5 μ M of each primer. qPCR was performed with paired technical replicates and with biological replicates of three or four as listed. Expression levels for genes were normalized

using β -actin as a control gene. Primers were made using the Primer 3 software. qPCR was performed in a Step One qPCR system (Thermo-Fisher). Relative mRNA expression levels were calculated using the $2-\Delta\Delta CT$ method. The following primers were used for amplification in 5' to 3' direction: F_Erbb4: CGCAGGCCAG TCTATGTAAT; R_Erbb4: TTAGTGGCTGAGAGGTTG GT; F_Erbb2: GGAACTTCTCCCCAGTATCC; R_Erbb2: CATGGAGGGTCTTTGATACC; F_Erbb1: GCCAAGTGA AACCAAAGTCC; R_Erbb1: CTTGGCGTGTTCTGGTAT TC; F_Erbb3: GCTACTGAACTCGGTGAGTG; R_Erbb3: GTCGGATCAGAGCTGTACCT; F_Nrg1: CGAGTGCTTT GTCCTCAAG; R_Nrg1: CAGCGATCACCAGTAAACTC; F_B Actin: AGAGGGGCTACAGCTTCACA; R_B Actin: GGAACCTCTCGTTGCCAATA.

4.9 | Statistics and software

JMP12 (SAS Institute Inc.) was used for data analysis. Data analysis were performed by calculating two tailed unequal variance student's (heteroscedastic) t test to test for significance; $P \le 0.05$ was considered significant and $P \le 0.01$ was considered highly significant. All error bars represent SE of the mean and center lines represent mean values.

ACKNOWLEDGEMENTS

We thank the Institute for Chemical Imaging of Living Systems at Northeastern University for consultation and imaging support. Thanks to David Stein for developing the computational HCR probe design pipeline. NSF grants 1558017 and 1656429 to JRM. Material and information obtained from the Ambystoma Genetic Stock Center funded through NIH grant: P40-OD019794. Andrew I Schafer Co-op Scholarship to TBJ. Northeastern Biochemistry Program financial support to TBJ.

AUTHOR CONTRIBUTIONS

Tyler Jensen: Conceptualization; data curation; formal analysis; funding acquisition; investigation; writingoriginal draft; writing-review & editing. Peter Giunta: Data curation; investigation. Natalie Schulz: Data curation; formal analysis; investigation. Jackson **Griffiths:** Data curation; formal analysis; investigation; writing-review & editing. Timothy Duerr: Data curation; formal analysis; investigation; writing-review & editing. Yaa Kyeremateng: Data curation; investigation. Hilary Wong: Data curation; investigation. Adeleso Adesina: Data curation; investigation. James Monaghan: Conceptualization; formal analysis; funding acquisition; investigation; methodology; project administration; supervision; writing-original draft; writing-review & editing.

CONFLICT OF INTEREST

The authors declare no potential conflict of interest.

ORCID

James R Monaghan https://orcid.org/0000-0002-6689-6108

REFERENCES

- 1. Koh Y. Update in acute respiratory distress syndrome. *J Intensive Care*. 2014;2(1):2. https://doi.org/10.1186/2052-0492-2-2.
- Hsia CC. Lessons from a canine model of compensatory lung growth. Curr Top Dev Biol. 2004;64:17-32. https://doi.org/10. 1016/s0070-2153(04)64002-6.
- 3. Gibney BC, Park MA, Chamoto K, et al. Detection of murine post-pneumonectomy lung regeneration by 18FDG PET imaging. *EJNMMI Research*. 2012;2(1):48. https://doi.org/10.1186/2191-219x-2-48.
- Butler JP, Loring SH, Patz S, Tsuda A, Yablonskiy DA, Mentzer SJ. Evidence for adult lung growth in humans. *N Engl J Med.* 2012;367(3):244-247. https://doi.org/10.1056/NEJMoa 1203983.
- Joven A, Elewa A, Simon A. Model systems for regeneration: salamanders. *Development*. 2019;146(14):1-4. https://doi.org/10. 1242/dev.167700.
- Farkas JE, Erler P, Freitas PD, Sweeney AE, Monaghan JR.
 Organ and appendage regeneration in the axolotl. In:
 Steinhoff G, ed. Regenerative Medicine—from Protocol to
 Patient: 1. Biology of Tissue Regeneration: Switzerland: Springer
 International Publishing; 2016:223-247.
- 7. Heath AG. Respiratory responses to hypoxia by *Ambystoma tigrinum* larvae, paedomorphs, and metamorphosed adults. *Comp Biochem Physiol A Comp Physiol*. 1976;55(1):45-49. https://doi.org/10.1016/0300-9629(76)90121-3.
- 8. Czopek J. Quantitative studies on the morphology of respiratory surfaces in amphibians. *Acta Anat.* 1965;62(2):296-323. https://doi.org/10.1159/000142756.
- 9. Dierichs R, Dosche C. The alveolar-lining layer in the lung of the axolotl, *Ambystoma mexicanum*. An electron-microscopic study using heavy metal complexes. *Cell Tissue Res.* 1982;222 (3):677-686. https://doi.org/10.1007/bf00213865.
- Scheuermann DW, Adriaensen D, Timmermans JP, de Groodt-Lasseel MH. Neuroepithelial endocrine cells in the lung of Ambystoma mexicanum. Anat Rec. 1989;225(2):139-149. https://doi.org/10.1002/ar.1092250209.
- Demircan T, İlhan AE, Aytürk N, Yıldırım B, Öztürk G, Keskin İ. A histological atlas of the tissues and organs of neotenic and metamorphosed axolotl. *Acta Histochem*. 2016;118(7): 746-759. https://doi.org/10.1016/j.acthis.2016.07.006.
- 12. Tanaka EM. The molecular and cellular choreography of appendage regeneration. *Cell.* 2016;165(7):1598-1608. https://doi.org/10.1016/j.cell.2016.05.038.
- 13. Buhain WJ, Brody JS. Compensatory growth of the lung following pneumonectomy. *J Appl Physiol*. 1973;35(6):898-902. https://doi.org/10.1152/jappl.1973.35.6.898.
- 14. Michalopoulos GK, MC DF. Liver regeneration. *Science*. 1997; 276(5309):60-66. https://doi.org/10.1126/science.276.5309.60.
- Ohashi A, Saito N, Kashimoto R, Furukawa S, Yamamoto S, Satoh A. Axolotl liver regeneration is accomplished via

- compensatory congestion mechanisms regulated by ERK signaling after partial hepatectomy. *Dev Dyn.* 2020;16. https://doi.org/10.1002/dvdy.262.
- Erler P, Sweeney A, Monaghan JR. Regulation of injury-induced ovarian regeneration by activation of Oogonial stem cells. Stem Cells. 2017;35(1):236-247. https://doi.org/10.1002/stem.2504.
- 17. Kotton DN, Morrisey EE. Lung regeneration: mechanisms, applications and emerging stem cell populations. *Nat Med.* 2014;20(8):822-832. https://doi.org/10.1038/nm.3642.
- 18. Basil MC, Katzen J, Engler AE, et al. The cellular and physiological basis for lung repair and regeneration: past, present, and future. *Cell Stem Cell*. 2020;26(4):482-502. https://doi.org/10.1016/j.stem.2020.03.009.
- Voswinckel R, Motejl V, Fehrenbach A, et al. Characterisation of post-pneumonectomy lung growth in adult mice. *Eur Respir J.* 2004;24(4):524-532. https://doi.org/10.1183/09031936.04. 10004904.
- Chen L, Acciani T, Le Cras T, Lutzko C, Perl AK. Dynamic regulation of platelet-derived growth factor receptor α expression in alveolar fibroblasts during realveolarization. *Am J Respir Cell Mol Biol.* 2012;47(4):517-527. https://doi.org/10.1165/rcmb. 2012-0030OC.
- Ysasi AB, Bennett RD, Wagner W, et al. Single-cell transcriptional profiling of cells derived from regenerating alveolar ducts. Front Med. 2020;7:112. https://doi.org/10.3389/fmed. 2020.00112.
- 22. Brody JS. Time course of and stimuli to compensatory growth of the lung after pneumonectomy. *J Clin Invest.* 1975;56(4):897-904. https://doi.org/10.1172/jci108169.
- 23. Brody JS, Burki R, Kaplan N. Deoxyribonucleic acid synthesis in lung cells during compensatory lung growth after pneumonectomy. *Am Rev Respir Dis.* 1978;117(2):307-316. https://doi.org/10.1164/arrd.1978.117.2.307.
- 24. Ding BS, Nolan DJ, Guo P, et al. Endothelial-derived angiocrine signals induce and sustain regenerative lung alveolarization. *Cell.* 2011;147(3):539-553. https://doi.org/10.1016/j.cell.2011.10.003.
- 25. Kaza AK, Laubach VE, Kern JA, et al. Epidermal growth factor augments postpneumonectomy lung growth. *J Thorac Cardiovasc Surg.* 2000;120(5):916-921. https://doi.org/10.1067/mtc. 2000.110460.
- Dao DT, Vuong JT, Anez-Bustillos L, et al. Intranasal delivery of VEGF enhances compensatory lung growth in mice. *PLoS One*. 2018;13(6):e0198700.
- 27. Kaza AK, Kron IL, Kern JA, et al. Retinoic acid enhances lung growth after pneumonectomy. *Ann Thorac Surg.* 2001;71(5): 1645-1650. https://doi.org/10.1016/s0003-4975(01)02478-x.
- Rafii S, Cao Z, Lis R, et al. Platelet-derived SDF-1 primes the pulmonary capillary vascular niche to drive lung alveolar regeneration. *Nat Cell Biol*. 2015;17(2):123-136. https://doi.org/ 10.1038/ncb3096.
- Kaza AK, Kron IL, Leuwerke SM, Tribble CG, Laubach VE. Keratinocyte growth factor enhances post-pneumonectomy lung growth by alveolar proliferation. *Circulation*. 2002;106 (12):I120-I124.
- 30. Liu Z, Wu H, Jiang K, et al. MAPK-mediated YAP activation controls mechanical-tension-induced pulmonary alveolar

- regeneration. *Cell Rep.* 2016;16(7):1810-1819. https://doi.org/10.1016/j.celrep.2016.07.020.
- 31. Vermeer PD, Einwalter LA, Moninger T, et al. Segregation of receptor and ligand regulates activation of epithelial growth factor receptor. *Nature*. 2003;422(6929):322-326. https://doi.org/10.1038/nature01440.
- 32. Vermeer PD, Panko L, Karp P, Lee JH, Zabner J. Differentiation of human airway epithelia is dependent on erbB2. *Am J Physiol Lung Cell Mol Physiol*. 2006;291(2):L175-L180.
- 33. Liu J, Kern JA. Neuregulin-1 activates the JAK-STAT pathway and regulates lung epithelial cell proliferation. *Am J Respir Cell Mol Biol.* 2002;27(3):306-313.
- Brechbuhl HM, Li B, Smith RW, Reynolds SD. Epidermal growth factor receptor activity is necessary for mouse basal cell proliferation. *Am J Physiol Lung Cell Mol Physiol*. 2014;307(10): L800.
- 35. Finigan JH, Downey GP, Kern JA. Human epidermal growth factor receptor signaling in acute lung injury. *Am J Respir Cell Mol Biol.* 2012;47(4):395-404.
- Yarden Y, Sliwkowski MX. Untangling the ErbB signalling network. Nat Rev Mol Cell Biol. 2001;2(2):127-137.
- 37. Brennan PJ, Kumogai T, Berezov A, Murali R, Greene MI. HER2/Neu: mechanisms of dimerization/oligomerization. *Oncogene*. 2000;19:6093.
- Britsch S. The neuregulin-I/ErbB signaling system in development and disease. Adv Anat Embryol Cell Biol. 2007;190:1-65.
- Mishra R, Foster DG, Finigan JH, Kern JA. Interleukin-6 is required for Neuregulin-1 induced HER2 signaling in lung epithelium. *Biochem Biophys Res Commun*. 2019;513(4):794.
- 40. Sudol M. Neuregulin 1-activated ERBB4 as a "dedicated" receptor for the hippo-YAP pathway. *Science Signaling*. 2014;7(355): pe29.
- 41. Lange AW, Sridharan A, Xu Y, Stripp BR, Perl AK, Whitsett JA. Hippo/yap signaling controls epithelial progenitor cell proliferation and differentiation in the embryonic and adult lung. *J Mol Cell Biol.* 2015;7(1):35-47.
- 42. Finigan JH, Mishra R, Vasu VT, et al. Bronchoalveolar lavage neuregulin-1 is elevated in acute lung injury and correlates with inflammation. *Eur Respir J.* 2013;41(2):396-401.
- 43. Farkas JE, Freitas PD, Bryant DM, Whited JL, Monaghan JR. Neuregulin-1 signaling is essential for nerve-dependent axolotl limb regeneration. *Development*. 2016;143(15):2724-2731.
- 44. Miller LD, Wert SE, Whitsett JA. Surfactant proteins and cell markers in the respiratory epithelium of the amphibian, *Ambystoma mexicanum. Comp Biochem Physiol A Mol Integr Physiol.* 2001;129(1):141-149.
- Rankin SA, Thi Tran H, Wlizla M, et al. A molecular atlas of Xenopus respiratory system development. *Dev Dyn.* 2015;244 (1):69-85.
- Liu W, Volpe MA, Zscheppang K, Nielsen HC, Dammann CE. ErbB4 regulates surfactant synthesis and proliferation in adult rat pulmonary epithelial cells. Exp Lung Res. 2009;35(1):29-47.
- 47. Plopper CG, St George JA, Read LC, et al. Acceleration of alveolar type II cell differentiation in fetal rhesus monkey lung by administration of EGF. *Am J Physiol*. 1992;262(3 Pt 1):L313-L321.
- 48. Purevdorj E, Zscheppang K, Hoymann HG, et al. ErbB4 deletion leads to changes in lung function and structure similar to

1101/gr.241901.118.

- bronchopulmonary dysplasia. Am J Physiol Lung Cell Mol Physiol. 2008;294(3):L516-L522.
- 49. Dammann CE, Nielsen HC, Carraway KL. Role of neuregulin-1 beta in the developing lung. *Am J Respir Crit Care Med.* 2003;167(12):1711-1716.
- Natarajan A, Wagner B, Sibilia M. The EGF receptor is required for efficient liver regeneration. *Proc Natl Acad Sci U S A*. 2007;104(43):17081-17086.
- 51. Bersell K, Arab S, Haring B, Kuhn B. Neuregulin1/ErbB4 signaling induces cardiomyocyte proliferation and repair of heart injury. *Cell*. 2009;138(2):257-270.
- 52. Zhang Y, Dube PE, Washington MK, Yan F, Polk DB. ErbB2 and ErbB3 regulate recovery from dextran sulfate sodium-induced colitis by promoting mouse colon epithelial cell survival. *Lab Invest*. 2012;92(3):437-450.
- 53. Sundvall M, Peri L, Maatta JA, et al. Differential nuclear localization and kinase activity of alternative ErbB4 intracellular domains. *Oncogene*. 2007;26(48):6905-6914.
- Farkas JE, Monaghan JR. Housing and maintenance of *Ambystoma mexicanum*, the Mexican axolotl. *Methods Mol Biol*. 2015;1290:27-46. https://doi.org/10.1007/978-1-4939-2495-0_3.
- 55. Beliveau BJ, Kishi JY, Nir G, et al. OligoMiner provides a rapid, flexible environment for the design of genome-scale oligonucle-otide in situ hybridization probes. *Proc Natl Acad Sci U S A*. 2018;115(10):E2183-e2192. https://doi.org/10.1073/pnas. 1714530115.
- Langmead B, Salzberg SL. Fast gapped-read alignment with bowtie 2. Nat Methods. 2012;9(4):357-359. https://doi.org/10. 1038/nmeth.

- 57. Smith JJ, Timoshevskaya N, Timoshevskiy VA, Keinath MC, Hardy D, Voss SR. A chromosome-scale assembly of the axolotl genome. *Genome Res.* 2019;29(2):317-324. https://doi.org/10.
- 58. Nowoshilow S, Schloissnig S, Fei JF, et al. The axolotl genome and the evolution of key tissue formation regulators. *Nature*. 2018;554(7690):50-55. https://doi.org/10.1038/nature25458.
- 59. Choi HMT, Schwarzkopf M, Fornace ME, et al. Third-generation in situ hybridization chain reaction: multiplexed, quantitative, sensitive, versatile, robust. *Development*. 2018;145 (12):1–10. https://doi.org/10.1242/dev.165753.
- 60. Schindelin J, Arganda-Carreras I, Frise E, et al. Fiji: an opensource platform for biological-image analysis. *Nat Methods*. 2012;9(7):676-682. https://doi.org/10.1038/nmeth.2019.
- 61. Schneider CA, Rasband WS, Eliceiri KW. NIH image to ImageJ: 25 years of image analysis. *Nat Methods*. 2012;9(7):671-675.
- 62. Stringer C, Wang T, Michaelos M, Pachitariu M. Cellpose: a generalist algorithm for cellular segmentation. *Nat Methods*. 2021; 18(1):100-106. https://doi.org/10.1038/s41592-020-01018-x.

How to cite this article: Jensen TB, Giunta P, Schultz NG, et al. Lung injury in axolotl salamanders induces an organ-wide proliferation response. *Developmental Dynamics*. 2021;250: 866–879. https://doi.org/10.1002/dvdy.315